# Optical properties and structure characterization of sapphire after Ni ion implantation and annealing

X. Xiang, X. T. Zu,[a] and J. W. Bao
*Department of Applied Physics, University of Electronic Science and Technology of China, Chengdu, People's Republic of China, 610054*

S. Zhu and L. M. Wang
*Department of Nuclear Engineering and Radiological Sciences, University of Michigan, Ann Arbor, Michigan 48109-2104*

(Received 17 January 2005; accepted 30 August 2005; published online 12 October 2005)

Implantation of 64 keV Ni ions to sapphire was conducted at room temperature to $1\times10^{17}$ ions/cm$^2$ with a current density of 5 or 10 $\mu$A/cm$^2$. Metallic Ni nanoparticles were formed with the 5 $\mu$A/cm$^2$ ion current and the $NiAl_2O_4$ compound was formed with the 10 $\mu$A/cm$^2$ ion current. The crystals implanted with both current densities were annealed isochronally for 1 h at temperatures up to 1000 °C in steps of 100 °C in an ambient atmosphere. Optical absorption spectroscopy, x-ray diffraction, transmission electron microscopy (TEM), and x-ray photoelectron spectroscopy have been utilized to characterize the samples. The surface plasmon resonance (SPR) absorption band peaked at 400 nm due to the Ni nanoparticles shifted toward the longer wavelength gradually with the annealing temperature increasing from 400 to 700 °C. The SPR absorption band disappeared after the annealing temperature reached 800 °C. NiO nanoparticles were formed at the expense of Ni nanoparticles with an increasing annealing temperature. The TEM analyses revealed that the nanoparticles grew to 6–20 nm and migrated toward the surface after annealing at 900 °C. The absorption band at 430 nm from $Ni^{2+}$ cations in $NiAl_2O_4$ did not shift with the increasing annealing temperature. © *2005 American Institute of Physics*. [DOI: 10.1063/1.2084314]

## INTRODUCTION

Nanostructured materials are promising to play a dominant role in future technology as they possess different, and often unique, properties relative to their macroscopic counterparts. Metallic nanoparticles embedded in insulators have been extensively studied because of pronounced optical effects, including surface plasmon resonance (SPR) absorption and strong third-order nonlinear optical (NLO) susceptibility.[1] These composites have drawn much attention due to applicability for all-optical-memory or switching devices and single electron transistors,[2–4] etc. The thermal stability of the metallic nanoparticles is particularly important for applications in optical devices that are subject to laser irradiations. In addition, the nucleation and growth of nanoparticles in ion-implanted substrates are affected by many parameters, such as ion fluence, current density (ion flux), implantation temperature, post-implantation annealing temperature, and atmosphere.[5–7] Fabrication and annealing effects on optical properties of metallic nickel nanoparticles embedded in silica glass have been studied.[8–10] Recently, we have fabricated metallic nickel nanoparticles embedded in a sapphire ($\alpha$-$Al_2O_3$) single crystal and observed a broad absorption band peaked at 400 nm, which has been ascribed to the surface plasmon resonance absorption of Ni nanoparticles.[11] In this paper, we report the effects of ion current density and thermal annealing on the formation process, microstructure, and optical properties of nanoparticles in a Ni ion-implanted sapphire. The as-implanted and annealed samples with different ion current densities and annealing temperatures were characterized by optical absorption, x-ray diffraction (XRD), transmission electron microscopy (TEM), and x-ray photoelectron spectroscopy (XPS) analyses.

## EXPERIMENTAL

Optical polished (0001) single crystals of sapphire, $10\times10\times0.5$ mm in dimensions, were implanted with Ni ions of 64 keV to a fluence of $1\times10^{17}$ ions/cm$^2$ in a vacuum chamber of $1.8\times10^{-3}$ Pa. The samples were kept at room temperature with a circulation of cooling water during ion implantation. The ion beam current density was controlled at 5 or 10 $\mu$A/cm$^2$. The samples were tilted off axis by approximately 7° to avoid channeling. After implantation, all the crystals turned gray and their transparency decreased. However, the transparency of crystals implanted at 10 $\mu$A/cm$^2$ was higher than that implanted at 5 $\mu$A/cm$^2$.

The $Ni^+$-implanted crystals with both current densities were then annealed isochronally for 1 h at temperatures up to 1000 °C in steps of 100 °C in ambient atmosphere in a quartz tube furnace. The heating rate was controlled at 10 °C/min. After ion implantation and each annealing step, the crystals were monitored using optical absorption spectroscopy. The optical absorption spectra were measured by a SHIMADZU UV-2550 spectrophotometer at room temperature, with a deuterium lamp for UV and a tungsten halogen lamp for the visible region. The wavelength used in the experiment ranged from 250 to 800 nm. X-ray diffraction spectra of some samples were collected using a Bede D1

[a]Author to whom correspondence should be addressed. Electronic mail: xiaotaozu@yahoo.com

 

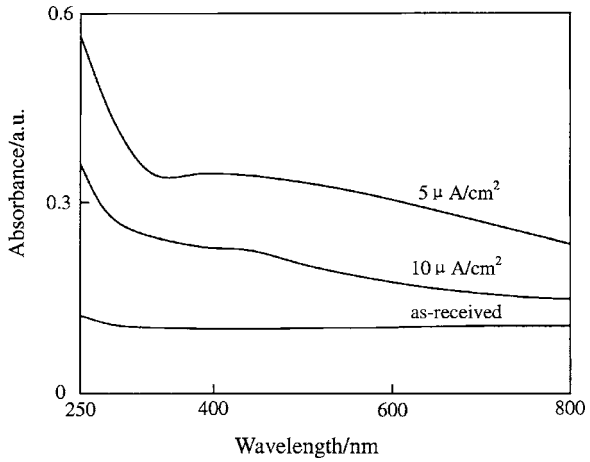


FIG. 1. Optical absorption spectra of as-received $Al_2O_3$ and Ni-implanted $Al_2O_3$ single crystals at different ion current densities.

type x-ray diffractometer with a Cu K$\alpha$ line of 1.54056 Å. A JEM 2010F field emission gun transmission electron microscope operating at 200 keV was used for the cross-sectional TEM analyses. X-ray photoelectron spectra of as-implanted samples were obtained at room temperature using a KRATOS X SAM 800 x-ray photoelectron spectrometer with monochromatic Al K$\alpha$ ($h\nu$=1486 eV). The $Ar^+$ ion beam etching of the sample surface was conducted with an ion energy of 3 keV and a current density of 10 $\mu$A/cm$^2$. The etching rate was approximately 1 nm/min.

## RESULTS AND DISCUSSION

The optical absorption spectra of as-received and as-implanted $Al_2O_3$ single crystals are shown in Fig. 1. The absorption spectrum of the pure crystal was a smooth line in the visible wave band due to a wide band gap ~9 eV. A broad absorption band peaked at 400 nm in the as-implanted crystal at a current density of 5 $\mu$A/cm$^2$ had been ascribed to the surface plasmon resonance absorption of Ni nanoparticles. The size of the Ni nanoparticles, 1–5 nm in diameter, had been proved by a TEM cross-sectional image in the previous study.[11] However, in the spectrum of an as-implanted crystal at a current density of 10 $\mu$A/cm$^2$, a narrower absorption band appeared at 430 nm.

Figure 2 shows the optical absorption spectra of annealed $Al_2O_3$ single crystals after Ni ion implantation with a current density of 5 $\mu$A/cm$^2$ and various annealing temperatures. As the annealing temperature increased, the absorption band shifted toward the longer wavelength and the gray color of crystals faded gradually. After annealing at 800 °C, this absorption band was absent. At the same time, the crystals turned colorless. However, a new absorption shoulder in the UV region began to appear after annealing at 600 °C. As the annealing temperature reached 800 °C, the UV absorption shoulder peak evolved into an absorption band and its peak position shifted to the longer wavelength of 306 nm (4.05 eV). There is no obvious change for the peak position of the absorption band after annealing at higher temperatures. However, the intensity of this absorption band decreased after annealing at temperatures above 800 °C. This

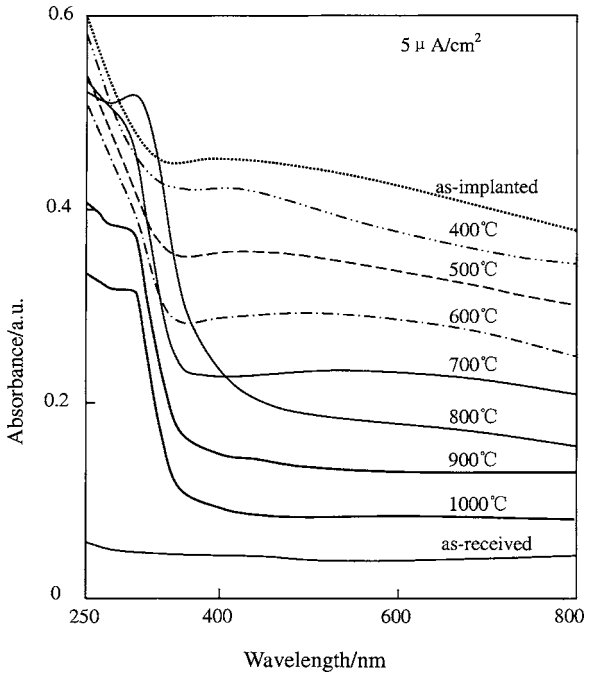


FIG. 2. Optical absorption spectra of annealed $Al_2O_3$ single crystals after Ni ion implantation with a current density of 5 $\mu$A/cm$^2$.

UV absorption band was probably related to the formation of a Ni oxide, presumably NiO, since NiO is an insulator with a band gap of ~4 eV (310 nm).[10] These assumptions have been verified by the following XRD measurements.

Figure 3 shows the spectra of annealed $Al_2O_3$ single crystals after Ni ion implantation at a current density of 10 $\mu$A/cm$^2$. There was no observable shift for the absorption band at 430 nm and the color of the crystals with the annealing temperature up to 900 °C. However, after annealing at 1000 °C, this absorption band disappeared and the crystal turned colorless immediately. In addition, there was

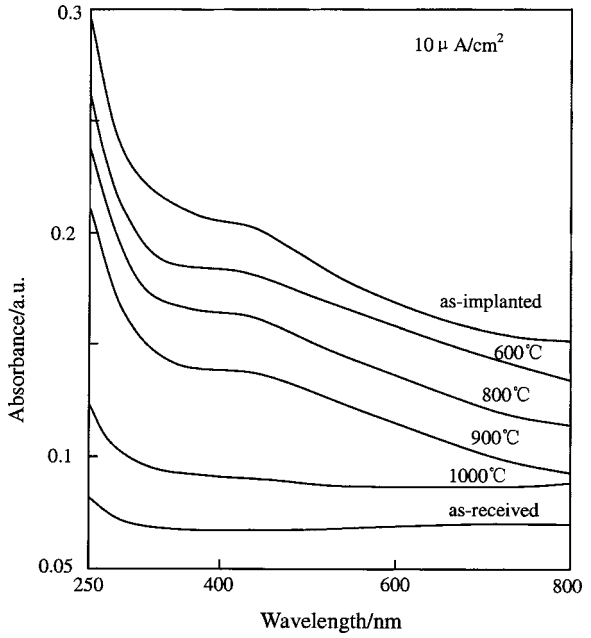


FIG. 3. Optical absorption spectra of annealed $Al_2O_3$ single crystals after Ni ion implantation at a current density of 10 $\mu$A/cm$^2$.

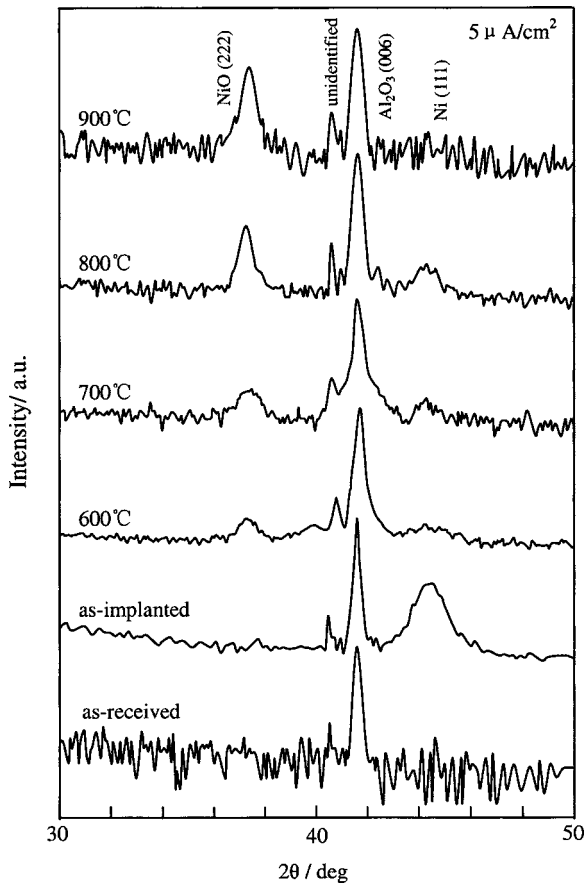


FIG. 4. XRD traces ($\theta$-$2\theta$) of an as-received and as-implanted $Al_2O_3$ crystal at a current density of 5 $\mu A/cm^2$ and annealed crystals at annealing temperatures from 600 to 900 °C.

no new absorption band appeared in the UV region for the annealed samples implanted at a current density of 10 $\mu A/cm^2$.

X-ray diffraction measurement was used to clarify the absorption bands of annealed crystals. Figure 4 shows XRD traces($\theta$–$2\theta$) of as-received and as-implanted crystal at a current density of 5 $\mu A/cm^2$ and annealed crystals at annealing temperatures from 600 to 900 °C. In all the spectra, two diffraction peaks can be observed at ~40.6° and ~41.7°, which were assigned to unidentified and (006) planes of the as-received $Al_2O_3$ crystals, respectively. The unidentified diffraction peak may be due to certain impurities in $Al_2O_3$ single crystals. For the as-implanted sample, a broad diffraction peak of metallic Ni appeared at ~44.3°, indicating that the dispersed metallic Ni formed Ni nanoparticles during ion implantation. This is consistent with the results of the previous study.[11] After annealing at 600 °C in air, the XRD peaks showed the coexisting spectra of both Ni and NiO nanoparticles diffraction peaks. As the annealing temperature increased, NiO nanoparticles grew at the expense of Ni nanoparticles. When the annealing temperature reached 900 °C, most of the Ni nanoparticles were oxidized into NiO nanoparticles. The trace of the Ni nanoparticles was hardly detectable, based on the XRD spectrum. These are in accordance with the absorption spectra of annealed samples (Fig. 3). Therefore, the UV absorption band peaked at ~306 nm is ascribed to the formation of NiO nanoparticles.

TABLE I. Average dimensions of Ni and NiO nanoparticles calculated from the XRD spectra of as-implanted and annealed $Al_2O_3$ crystals after Ni ion implantation with an ion current density of 5 $\mu A/cm^2$.

| Samples | Ni particle size (nm) | NiO particle size (nm) |
|---|---|---|
| As-implanted | 4.9 | — |
| Annealed at 600 °C | 5.1 | 10.8 |
| Annealed at 700 °C | 5.5 | 11.6 |
| Annealed at 800 °C | 9.2 | 19.9 |
| Annealed at 900 °C | — | 21.5 |

In order to evaluate the mean grain size of Ni and NiO nanoparticles, the Scherrer formula[12] was used:

$$D = \frac{0.9\lambda}{B\cos(\theta_B)},$$

where $\lambda$, $\theta_B$, and $B$ are the x-ray diffraction wavelength (1.54056 Å), Bragg diffraction angle, and the full width at half-maximum (FWHM) of diffraction peaks, respectively. The calculated grain sizes of Ni and NiO nanoparticles were listed in Table I for as-implanted and annealed samples. The Ni nanoparticles with a mean dimension of 4.9 nm is consistent with the previous TEM result, up to 5 nm in diameter, in as-implanted samples.[11] The annealing effect on the growth of Ni nanoparticles was small up to 800 °C, which is similar to Ni nanoparticles in silica glass.[13] The growth of NiO nanoparticles mainly occurred at an annealing temperature above 800 °C. These results just explained the shift toward the longer wavelength of the UV absorption band, i.e., the optical band gap of NiO nanoparticles shifted toward lower energy due to the quantum confinement effect as the grain size increased.

Figure 5 shows a cross-sectional bright field (BF) and a high-resolution TEM image from the sample annealed at 900 °C after Ni ion implantation with a current density of 5 $\mu A/cm^2$. In the BF image [Fig. 5(a)], the nanoparticles grew to 6–20 nm in diameter with irregular shapes, which is consistent with the XRD result. In addition, the nanoparticles migrated toward the surface of the crystal after annealing. A high density of voids formed below the nanoparticles during the thermal annealing process. The amorphous area of the $Al_2O_3$ matrix was partially recrystallized after the annealing. The HRTEM image [Fig. 5(b)] demonstrates the single crystalline nature of the NiO nanoparticle.

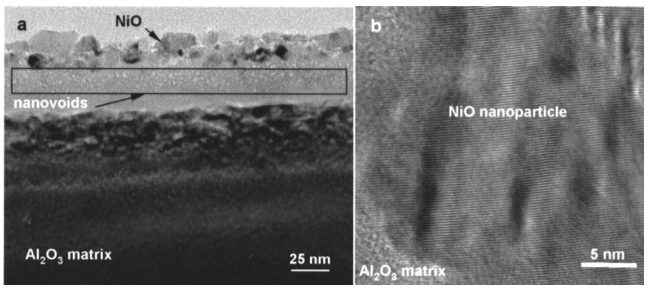


FIG. 5. A cross-sectional bright-field and a high-resolution TEM image from a sample annealed at 900 °C after Ni ion implantation with a current density of 5 $\mu A/cm^2$.

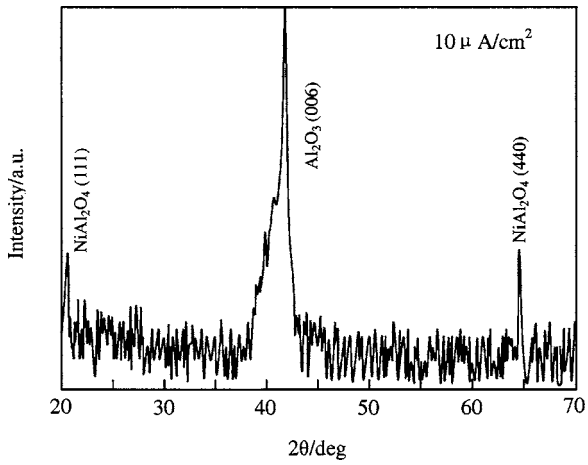


FIG. 6. XRD traces ($\theta$–$2\theta$) of an as-implanted $Al_2O_3$ crystal at a current density of 10 $\mu A/cm^2$.

Figure 6 shows XRD traces ($\theta$–$2\theta$) of an as-implanted crystal at a current density of 10 $\mu A/cm^2$. After ion implantation, two new diffraction peaks appeared at ~20.58° and ~64.56°, respectively. According to the JCPDS card (No. 78-1601), these two diffraction peaks may be corresponding to (111) and (440) planes ($2\theta$=19.08° and 65.545°) of $NiAl_2O_4$. The peak shifts with respect to the powder diffraction data may suggest an existing stress due to the lattice distortion after the Ni ion implantation.

In order to prove the formation of a $NiAl_2O_4$ compound, XPS measurements were conducted. The sample had been etched 2 nm with an $Ar^+$ ion before measurements in order to remove surface contamination. Figure 7 shows the XPS spectra of the $Ni_{2p3/2}$ core level of the as-implanted crystal at a current density of 10 $\mu A/cm^2$. The $C_{1S}$ peak at 285.0 eV is used to calibrate the spectra. For the sake of clarity, the $Ni_{2p3/2}$ region is presented as resolved into Gaussian components. The peak at a binding energy (BE) of 856.6 eV can be attributed to $Ni^{2+}$ in $NiAl_2O_4$ and the one at 862.8 eV is assigned to the well-known shake-up satellite peak of $Ni^{2+}$. The two peak positions and their energy difference 6.2 eV are just consistent with the previous study.[14] Thus, the XPS result further proved the formation of $NiAl_2O_4$ with the spinel structure.

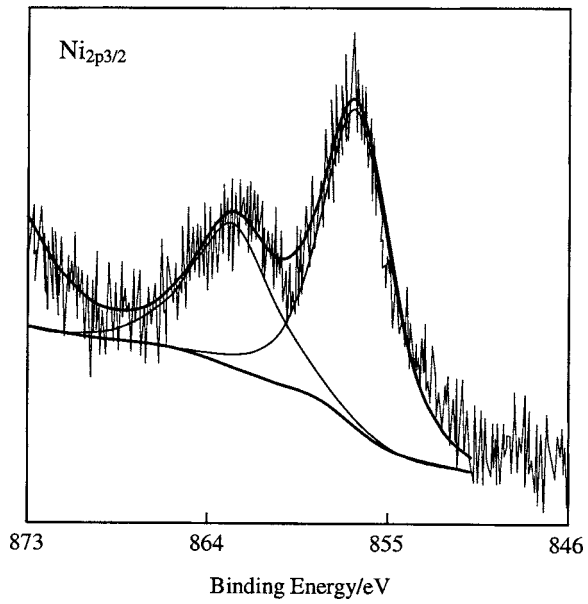


FIG. 7. XPS spectra of $Ni_{2p3/2}$ core level of the as-implanted crystal at a current density of 10 $\mu A/cm^2$.

Based on the XRD and XPS analyses, it can be concluded that there is no Ni nanoparticle formation after Ni ion implantation at a current density of 10 $\mu A/cm^2$, i.e., the absorption band at 430 nm may be related to $Ni^{2+}$ cations within the $NiAl_2O_4$ spinel structure rather than the SPR absorption of metallic Ni nanoparticles. This suggests that the formation of metallic Ni nanoparticles in sapphire single crystals is very sensitive to the ion current density just as the Cu nanoparticle formation in silica glass.[5] The ion current density of 5 $\mu A/cm^2$ may be a proper implantation parameter to form Ni nanoparticles in sapphire at room temperature. The growth of metallic Ni nanoparticles mainly occurred at an annealing temperature of ~800 °C in samples after ion implantation at a current density of 5 $\mu A/cm^2$. The SPR absorption band shifted toward the longer wavelength gradually due to the slight growth of nanoparticles with the annealing temperature increasing from 400 to 700 °C. However, the SPR band disappeared after the size of Ni nanoparticles reached 9.2 nm at ~800 °C. Unlike the SPR absorption of Ni nanoparticles, the absorption band of $Ni^{2+}$ cations in $NiAl_2O_4$ did not shift with the increasing annealing temperatures. NiO is an antiferromagnetic insulator and its formation by means of ion implantation and annealing has been reported in Ni negative ion-implanted $SiO_2$ and Ni positive ion-implanted YSZ.[10,15] However, the annealing atmosphere was $O_2$ gas for $SiO_2$ and air for sapphire. It seems that the Ni nanoparticles are easy to be oxidized in sapphire as compared with that in $SiO_2$.

## CONCLUSION

Metallic Ni nanoparticles formed in sapphire after 64 keV Ni ion implantation to $1\times10^{17}$ ions/$cm^2$ with an ion current density of 5 $\mu A/cm^2$ at room temperature. However, $NiAl_2O_4$ compound formed after implantation with a current density of 10 $\mu A/cm^2$. In the samples implanted with the lower ion current density (5 $\mu A/cm^2$), the SPR absorption band peaked at 400 nm due to the Ni nanoparticles shifted toward the longer wavelength gradually with the annealing temperature increasing from 400 to 700 °C. The SPR absorption band disappeared after the annealing temperature reached 800 °C. NiO nanoparticles formed at the expense of Ni nanoparticles with the increasing annealing temperature. The TEM analyses showed that the nanoparticles grew to 6–20 nm and migrated toward the surface after annealing at 900 °C. The absorption band at 430 nm of $Ni^{2+}$ cations in $NiAl_2O_4$ did not shift with the increasing annealing temperatures.

## ACKNOWLEDGMENTS

This study was supported financially by the NSAF Joint Foundation of China (Grant No. 10376006) and by the U.S. Department of Energy under Grant No. DF-FG02-02ER46005. We also thank the Program for New Century

Excellent Talents in University and the Sichuan Young Scientists Foundation (Grant No. 03ZQ026-059).

[1]A. Meldrum, R. F. Haglund, Jr., L. A. Boatner, and C. W. White, Adv. Mater. (Weinheim, Ger.) **13**, 1431 (2001).
[2]L. Yang, D. H. Osborne, R. F. Haglund, Jr., R. H. Magruder, C. W. White, R. A. Zuhr, and H. Hosono, Appl. Phys. A: Solids Surf. **62**, 403 (1996).
[3]P. Chakraborty, J. Mater. Sci. **33**, 2235 (1998).
[4]A. Nakajima, H. Nakao, H. Ueno, T. Futatsugi, and N. Yokoyama, Appl. Phys. Lett. **73**, 1071 (1998).
[5]O. A. Plaksin, Y. Takeda, N. Okubo, H. Amekura, K. Kono, N. Umeda, and N. Kishimoto, Thin Solid Films **464-465**, 264 (2004).
[6]J. L. Chen, R. Mu, A. Ueda, M. H. Wu, Y. S. Tung, Z. Gu, D. O. Henderson, C. W. White, J. D. Budai, and R. A. Zuhr, J. Vac. Sci. Technol. A **16**, 1409 (1998).
[7]Y. X. Liu, Y. C. Liu, D. Z. Shen, G. Z. Zhong, X. W. Fan, X. G. Kong, R. Mu, and D. O. Henderson, Solid State Commun. **121**, 531 (2002).
[8]T. Isobe, S. Y. Park, and R. A. Weeks, J. Non-Cryst. Solids **189**, 173 (1995).
[9]H. Amekura, H. Kitazawa, N. Umeda, Y. Takeda, and N. Kishimoto, Nucl. Instrum. Methods Phys. Res. B **222**, 122 (2004).
[10]H. Amekura, N. Umeda, Y. Takeda, J. Lu, and N. Kishimoto, Appl. Phys. Lett. **85**, 1015 (2004).
[11]X. Xiang, X. T. Zu, S. Zhu, and L. M. Wang, Appl. Phys. Lett. **84**, 52 (2004).
[12]B. D. Cullity, *Elements of X-Ray of Diffractions* (Addition-Wesley, Reading, MA, 1978), p. 102.
[13]H. Amekura, Y. Takeda, and N. Kishimoto, Nucl. Instrum. Methods Phys. Res. B **222**, 96 (2004).
[14]J. Słoczyński, J. Ziółkowski, B. Grzybowska, R. Grabowski, D. Jachewicz, K. Wcisło, and L. Gengembre, J. Catal. **187**, 410 (1999).
[15]X. Xiang, X. T. Zu, S. Zhu, and L. M. Wang, Physica B **368**, 88 (2005).